

1
2
3
4
5
6
7
8
9
10
11
12
13
14
15
16
17
18
19
20
21
22
23
24
25
26
27
28
29
30
31
32
33
34
35
36
37
38

Stavudine Reduces NLRP3 Inflammasome Activation and Upregulates A β -Autophagy

**Francesca La Rosa^{1*}, Marina Saresella¹, Ivana Marventano¹, Federica Piancone¹,
Enrico Ripamonti¹, Chiara Paola Zoia^{2,3}, Elisa Conti^{2,3}, Carlo Ferrarese^{2,3,4}, Mario Clerici^{1,5}**

¹ Don C. Gnocchi Foundation, Istituto di Ricovero e Cura a Carattere Scientifico (IRCCS), 20128 Milan, Italy

² Laboratory of Neurobiology, School of Medicine and Surgery, 20900 Monza, Italy, ³ Milan Center for Neuroscience, Milano, University of Study of Milano-Bicocca, 20126 Milan, Italy

⁴ Department of Neuroscience, S. Gerardo Hospital, 20052, Monza, Italy.

⁵ University of Milan, 20122 Milan, Italy.

* Corresponding Author

*Francesca La Rosa PhD
Laboratory of Molecular Medicine and Biotechnology
Don Gnocchi Foundation ONLUS IRCCS
via Capecelatro, 66
20148 Milano
Tel +390240308374
Fax +390240308438
Email: flarosa@dongnocchi.it*

Running Title: D4T reduces NLRP3 activation

39

40

ABSTRACT

41

42

43 Alzheimer's disease (AD) is associated with amyloid-beta ($A\beta$) deposition and neuroinflammation,
44 possibly driven by activation of the NLRP3 inflammasome. Nucleoside reverse transcriptase
45 inhibitors (NRTI) hamper the assembly of the NLRP3 inflammasome; we analyzed whether
46 stavudine (D4T), a prototypical NRTI, modulates $A\beta$ -mediated inflammasome activation; because
47 neuroinflammation impairs $A\beta$ clearance by phagocytes, phagocytosis and autophagy were
48 examined as well. THP-1-derived macrophages were stimulated *in vitro* with $A\beta_{42}$ alone or after
49 LPS priming with/without D4T. NLRP3 and TREM2 expression was analyzed by RT-PCR,
50 phagocytosis and ASC-Speck by AmnisFlowSight, NLRP3-produced cytokines by ELISA,
51 autophagy by P-ELISA evaluation of P-ERK and P-AKT. Results showed that IL1 β , IL18 and
52 caspase-1 were increased whereas $A\beta$ -phagocytosis and TREM2 were reduced in LPS+ $A\beta_{42}$ -
53 stimulated cells. D4T reduced NLRP3 assembly as well as IL18 and caspase-1 production, but not
54 IL1 β , phagocytosis, and TREM2. P-AKT expression was augmented and P-ERK was reduced by
55 D4T, suggesting a stimulatory effect on autophagy. D4T reduces NLRP3 inflammasome-associated
56 inflammation, possibly restoring autophagy, in an *in vitro* model of AD; it will be interesting to
57 verify its possibly beneficial effects in the clinical scenario.

58

59 .

60

61

62

63

64

65

66

67

INTRODUCTION

68

69 Alzheimer's disease is a neurodegenerative pathology associated with the deposition of
70 extracellular amyloid beta (A β) plaques within the brain. Oligomeric A β -deposition is held
71 responsible for the activation of microglia, which results in the production of several neurotoxic
72 molecules including inflammatory cytokines, ultimately leading to neurotoxicity, progressive
73 synaptic loss, and cognitive decline (Town *et al*, 2001; Tan *et al*, 2002; Town *et al*, 2005;
74 Townsend *et al* 2005; Simard *et al*, 2006; Town *et al*, 2008; Fiala & Veerhuis, 2010; Feng *et al*,
75 2011; Heneka *et al*, 2015a).

76 Inflammation has convincingly been demonstrated to be a key driver of the disease (Tuppo & Arias
77 2005; Griffin *et al*, 2006; Cai *et al*, 2014; Wanga *et al*, 2017), and recent results suggest that the
78 activation of the nod-like receptor protein 3 (NLRP3) inflammasome is responsible for such
79 inflammation. This is based on a number of observations, thus: 1) the concentration of the
80 inflammasome-derived proinflammatory cytokines interleukin (IL)-1 β and IL-18 is increased in AD
81 (Heneka *et al*, 2013; Gold & El Khoury, 2015; Saresella *et al*, 2016; Awad *et al*, 2017); 2) NLRP3-
82 deficiency in the APP/PS1 mouse model of AD decreases neuroinflammation and A β accumulation
83 and improves neuronal function (Heneka *et al*, 2013); and 3) higher IL-1 β concentrations are
84 detected in individuals with a diagnosis of amnesic mild cognitive impairment (aMCI) that convert
85 into AD (La Rosa *et al*, 2018). Notably, NLRP3 up-regulation is now recognized as a central
86 component in the development of several inflammatory and autoimmune diseases (Lamkanfi *et al*,
87 2012; Strowig *et al*, 2012; Guo *et al*, 2015).

88 In AD A β accumulation is initially contrasted by the activation of phagocytic cells. In the long run
89 though, these cells become engulfed by A β peptides; this leads to the release of cathepsin B, which
90 further stimulates the activation of the NLRP3 inflammasome (Halle *et al*, 2008). This process is
91 contrasted by the action of triggering receptor expressed on myeloid cells 2 (TREM2), a protein that
92 plays a protective role in AD by inhibiting the inflammatory response, enhancing A β phagocytosis
93 (Hamerman *et al*, 2006; Casati *et al*, 2018), and promoting microglial functions in response to A β
94 deposition (Bouchon *et al*, 2001; Klesney-Tait *et al*, 2006; Neumann & Takahashi, 2007;

95 Bajramovic 2011; Colonna & Wang 2016; Tan *et al*, 2017). The A β accumulation-associated
96 phagocytosis defect also jeopardizes the activity of the autophagic flux (Fiala *et al*, 2005; Hui *et al*,
97 2017). This is important in AD, as alterations of autophagy, a process that mediates lysosomal
98 degradation of proteins, inflammatory cells and organelles, were shown to play a pathogenic role in
99 this disease (Uddin *et al*, 2018). Thus, recent data showed that the degradation of extracellular A β
100 by microglia is dependent on autophagic processes, and that autophagy is important for the
101 regulation of A β -mediated NLRP3 activation (Rodgers *et al*, 2014; Qian *et al*, 2017).

102 The mechanism linking autophagy and NLRP3 activation was clarified by observations indicating
103 that autophagy down regulates NLRP3 via the induction of a lysine 63-linked ubiquitination of the
104 NLRP3 adaptor molecule ASC (Shi *et al*, 2012); the autophagosome engulfs these substrates and
105 eliminates them after fusion with the lysosome (Harris *et al*, 2011). Hence, autophagy disrupts
106 multiple steps of inflammasome activation to prevent excessive inflammation (Harris *et al*, 2011;
107 Ferguson TA & Green, 2014; Saitoh *et al*, 2014); The exact intracellular signaling mechanisms
108 involved in the regulation of autophagy are still to be elucidated, but a pivotal role for two MAP-
109 kinases: ERK and AKT, is strongly suspected (Martinez-Lopez *et al*, 2013; Joassard *et al*, 2013).
110 Thus, ERK1 phosphorylation (ERK-P) activates mTOR and, as a consequence, inhibits autophagy;
111 conversely the phosphorylation of AKT (AKT-P) inhibits mTOR (Hay 2005; Peng *et al*, 2010) and
112 activates autophagosomes through chaperone-mediated (LAMP) autophagy (Yang & Klionsky,
113 2010; Heras-Sandoval *et al*, 2014; Li *et al* 2017). Of note, ERK1/2 phosphorylation was recently
114 shown to inhibit the NLRP3 inflammasome (Mezzasoma *et al*, 2017), and ERK-P was
115 demonstrated to associate with A β accumulation in an AD animal model (Jin *et al* 2012).

116 These observation, together with data implying that inflammasome activation impacts on the risk of
117 developing AD, suggest that targeting inflammation and, in particular, the activation of the NLRP3
118 inflammasome, could positively modulate A β phagocytosis and autophagy, possibly offering a
119 therapeutic opportunity. Recent results showed that nucleoside reverse transcriptase inhibitors,
120 including stavudine (D4T), one of the compounds initially used in the therapy of HIV infection,
121 inhibit the activation of the inflammasome and prevents the transcription of proteins that are part of
122 the inflammasome complex (Kerur *et al*, 2013; Fowler *et al*, 2014;). These results suggest a
123 possible beneficial role of D4T in inflammatory diseases, including AD. We verified this hypothesis
124 in an *in vitro* system using THP-1-derived macrophages.

RESULTS

125

126

127 *Cellular toxicity of D4T*

128 To determine the optimal dose of D4T to be used in the experiments, two different doses of the
129 drug (50 μ M and 100 μ M) were added to cell cultures of THP-1-derived macrophages; cell
130 viability was analyzed using the MTT assay. Results showed that, whereas the higher dose of D4T
131 significantly reduced the viability of cells compared to control (medium alone); the lower dose of
132 drug had only a marginally effect on this parameter as >90% of cells were viable at the end of the
133 incubation period (data not shown). Based on these results, the dose of 50 μ M D4T was used in all
134 the experiments.

135

136 *D4T reduces mRNA expression of NLRP3 proteins in THP-1-derived macrophages*

137 Quantitative PCR analyses were performed in THP-1-derived macrophages that were stimulated
138 with A β ₄₂ alone or with A β ₄₂ after priming with LPS; analyses were performed in the
139 absence/presence of D4T. Stimulation in both conditions: A β ₄₂ alone or A β ₄₂ after priming with
140 LPS, resulted in a significant upregulation of the mRNA expression of all the proteins that are part
141 of the NLRP3 inflammasome complex, reinforcing the idea that A β ₄₂ accumulation results in
142 NLRP3 activation-driven inflammation (Fig 1).

143 Notably, D4T was able to significantly reduce the mRNA expression of the sensor (Nlrp3), adaptor
144 (ASC), and effectors (IL-1 β and IL-18) proteins that compose the NLRP3 inflammasome ($p <$
145 0.005 in all cases). In contrast with these results, D4T did not reduce but rather increased mRNA
146 expression of the catalytic NLRP3 inflammasome proteine caspase-1 (Fig 1).

147

148 *Effect of D4T on NLRP3-associated production of pro-inflammatory cytokines*

149 The production of the NLRP3 activation-related proinflammatory cytokines IL-1 β and IL-18, as
150 well as that of caspase-1, was measured next in THP-1-derived macrophages that were stimulated
151 with A β ₄₂ alone or with A β ₄₂ after priming with LPS in the absence/presence of D4T.

152 Results showed that the production of all these proteins was up regulated in both A β ₄₂-stimulated
153 and LPS+A β ₄₂-stimulated cells ($p < 0.05$ in all cases), with the highest protein production being
154 observed in LPS+A β ₄₂-stimulated cells.

155 The addition of D4T significantly reduced IL-18 and caspase-1 production in all the examined
156 experimental conditions ($p < 0.005$ in all cases); the drug significantly down regulated IL-1 β
157 production by A β ₄₂-stimulated THP-1-derived macrophages alone as well ($p < 0.005$), but it had a
158 marginal effect, or, paradoxically, it increased IL-1 β production by LPS+A β ₄₂-stimulated cells.
159 These results are shown in Figure 2.

160

161 ***D4T inhibits NLRP3/ASC-speck inflammasome assembly***

162 The effect of D4T on NLRP3 inflammasome activation was verified next in THP-1-derived
163 macrophages that were stimulated in the same experimental conditions by using the Amnis Flow
164 Sight technology. Representative images are provided in figures 3, panels A-through-C. Results
165 confirmed that, as compared to what observed in cells stimulated with A β ₄₂ alone (Fig 3A),
166 LPS+A β ₄₂ stimulation causes a much more extensive assembly of NLRP3 and ASC within large
167 protein complexes (specks), which are the result of inflammasome activation (Fig 3B). Results also
168 showed that D4T prevents the generation of specks, hence impeding the assembly of the NLRP3
169 inflammasome (Fig 3C). Figure 3D shows overall results that can be summarized as follows: 1)
170 NLRP3 ASC-speck colocalization (assembly of inflammasome) is significantly increased in
171 LPS+A β ₄₂ compared to A β ₄₂ alone-stimulated cells ($p = 0.0001$); 2) D4T significantly reduces
172 NLRP3/ASC-speck colocalization (assembly of inflammasome) in LPS+A β ₄₂ activated cells ($p =$
173 0.007).

174

175 ***D4T modulation of A β ₄₂ phagocytosis by THP-1-derived macrophages***

176 The phagocytic ability of THP-1-derived macrophages that were stimulated with A β ₄₂ alone or with
177 A β ₄₂ after priming with LPS in the absence/presence of D4T was measured next. Results showed
178 that NLRP3 activation was correlated with a significantly reduced ability of these cells to phagocyte
179 A β ₄₂ ($p \leq 0.05$ in all condition), suggesting that NLRP3 inflammasome-related inflammation plays
180 a role in the impairment of phagocytosis seen in AD. Results also showed that addition of D4T to

181 cell cultures could not restore the impairment of A β ₄₂ phagocytosis by THP-1-derived macrophages
182 in any of the analyzed experimental conditions ($p < 0.05$ in all condition). These results are shown
183 in Figure 4.

184

185 ***D4T modulation of TREM-2 mRNA expression***

186 To determine the relationship between NLRP3-activation and A β -phagocytosis we also evaluated
187 TREM-2 mRNA expression in all experimental conditions. Results showed a significant reduction
188 of TREM-2 mRNA in LPS +A β ₄₂ compared to A β ₄₂ alone stimulated cells ($p \leq 0.001$). When the
189 effect of D4T on TREM-2 expression was analyzed, results indicated that TREM-2 was reduced by
190 D4T in all the examined conditions. ($p \leq 0.001$) (Fig 5), further confirming that this compound does
191 not have an effect on phagocytosis.

192

193 ***D4T-modulation of ERK e AKT- phosphorylation and autophagy***

194 D4T did not modulate A β -phagocytosis, but the action of an alternate phagocytic pathway,
195 autophagy, was repeatedly shown to play a primary role in A β degradation by the microglia. We
196 thus analyzed the relative activation of these two phagocytic pathways by evaluating the
197 phosphorylation status of ERK and AKT.

198 Result showed that phosphorylation of these two proteins was significantly modulated by D4T in
199 protein extracts of THP-1-derived macrophages. Thus: 1)D4T resulted in a significant up-regulation
200 of AKT phosphorylation in all conditions ($p < 0.05$ in all conditions); 2) in the same protein
201 extracts, p-ERK was significantly decreased by D4T in all the examined experimental conditions (p
202 ≤ 0.001 for all comparison) (Fig 6).

203

204

205

206

207

208

DISCUSSION

209

210 Inflammasomes are fundamental intracellular structures formed by a number of proteins whose
211 assembly results in inflammation. An exaggerated and persistent activation of the NLRP3
212 inflammasome, though, has repeatedly been shown to play a pivotal role in autoimmune and
213 inflammatory diseases including AD. The involvement of NLRP3 inflammasome in AD, in
214 particular, is supported by results obtained both in patients and in animal models, including the
215 observations that the concentration of IL-1 β and IL-18, prototypical NLRP3-produced proteins, is
216 increased in AD (Heneka *et al*, 2013; Gold & El Khoury, 2015; Saresella *et al*, 2016; Awad *et al*,
217 2017) and that NLRP3-deficiency in the APP/PS1 mouse model of AD decreases
218 neuroinflammation and A β accumulation and improves neuronal function (Heneka *et al*, 2013).
219 Further support to the involvement of the NLRP3 inflammasome in the pathogenesis of AD was
220 offered by results showing that A β induces the processing of pro-IL-1 β into mature IL-1 β in the
221 microglia via activation of NLRP3 inflammasome (Parajuli *et al*, 2013), and that NLRP3
222 inflammasome deficiency favors the differentiation of microglia cells into the M2 phenotype
223 (anti-inflammatory) (Hu *et al*, 2015; Dempsey *et al*, 2017). Neuroinflammation also impacts on the
224 ability of the phagocytes to eliminate A β peptides, and in AD it is well known that an impairment in
225 the ability of phagocytes to catabolize A β peptides leads to the engulfment and the functional
226 paralysis of these cells, favoring the accumulation of A β and its deposition in plaques. We used an
227 *in vitro* system to analyze the involvement of NLRP3 inflammasome activation in A β -
228 phagocytosis and to verify whether the dampening of inflammasome activation would result in a
229 stimulation of autophagy. To this end we used Stavudine (D4T) an antiviral designed to target HIV
230 reverse transcriptase, that was recently shown to be endowed with the ability of down modulating
231 NLRP3 inflammasome activation. Data herein, obtained using an *in vitro* model of AD and
232 methods that allow single cell direct visualization by merging flow cytometry and high-resolution
233 microscopy, show that the NLRP3 inflammasome activation is directly correlated with the
234 impairment in phagocytosis that characterizes AD. We also demonstrate that D4T, an antiviral that
235 has been widely used in the therapy of HIV infection, greatly reduces NLRP3 inflammasome
236 activation and, whereas it does not have an effect on phagocytosis, it could significantly upregulate
237 A β autophagy by macrophages.

238 D4T down regulated the expression of all NLRP3 proteins mRNA with the exception of caspase-1
239 This is possibly the result of a moderate activation of mRNA caspase-1 by LPS priming, or,
240 alternatively, it could be driven by the spontaneous release of endogenous ATP (Netea *et al*,2009).
241 Similarly, the drug reduced the production of IL-18 but not of IL1 β ; this discrepancy can be
242 justified by the observation that, whereas IL-18 is a purely NLRP3 activation-derived cytokine, IL-
243 1 β can be secreted by monocytes independently of classical inflammasome stimuli (Gaidt *et al*,
244 2016). A β clearance is a complex, multifactorial process, requiring the collaboration of various
245 systems and cell types, including microglia, macrophages and peripheral monocytes (Zuroff *et al*,
246 2017). Notably, whereas it is still unclear whether A β accumulation is a cause or consequence of
247 disease, mounting evidences have shown that increased cerebral A β burden is the earliest
248 pathologic event in AD, supporting the idea that A β accumulation plays a principal role in this
249 disease. Clearance of A β is believed to be hampered as a consequence of inflammation. Our data
250 showing a significant reduction of A β -phagocytosis in THP-1 derived macrophages that were
251 preactivated with LPS (inflammatory condition) compared to those cultured with A β alone (non-
252 inflammatory condition) support this idea. Notably, thou, whereas D4T could greatly reduce
253 NLRP3 inflammasome activation, this compound did not have any effect of phagocytosis in the *in*
254 *vitro* experimental model we used. The lack of effect of D4T on phagocytosis was further
255 reinforced by the observation that the expression of TREM2, a receptor that is expressed on
256 microglial/macrophages cells (Jones *et al*, 2014) and acts as a sensor for A β clearance, was not
257 modulated either by this compound. This discrepancy could be explained in different ways: 1) A β
258 phagocytosis is independent from NLRP3 activation; 2) other, yet unknown mechanisms impair
259 phagocytosis even when NLRP3 activation is impeded; 3) our system does not represent what goes
260 on *in vivo*. An alternate and more interesting explanation stems from a number of recent results
261 suggesting that successful A β clearance in AD is mediated not by phagocytosis but, rather, by
262 autophagy: a process that mediates lysosomal degradation of proteins, inflammatory cells and
263 organelles.

264 Autophagy and NLRP3 inflammasome activation have indeed been linked by the observation that
265 autophagy down regulates NLRP3 *via* the induction of a lysine 63-linked ubiquitination of ASC
266 and, on the other hand, autophagy inhibition exacerbates inflammasome activity and disease in

267 models of influenza infection, and autoimmune conditions including IBD (Nakahira *et al*, 2011;
268 Lupfer *et al* 2013; Ravindran *et al* , 2016).

269 Autophagy is a complex metabolic mechanism that includes a number of pathways, the best
270 characterized of which are microautophagy, which is mediated by the phosphorylation of AKT, and
271 LAMP chaperone-mediated autophagy (Kiffin *et al*, 2004; Vernon & Tang, 2013). We observed
272 that, in concomitance with its dampening effect on NLRP3 activation, D4T resulted in a significant
273 increase of phosphorylated AKT. AKT phosphorylation modulates mTOR signaling pathway and
274 LAMP chaperon-mediated autophagy. These results confirm, at least in the *in vitro* system we used,
275 that D4T could have a beneficial effect on stimulating autophagy-mediated A β clearing possibly as
276 a consequence of its ability to reduce NLRP3 inflammasome activation. These data could be
277 important in the light of observations in the animal model of AD showing that, in autophagy
278 deficient mice, accumulation of A β is seen in brain cells and results in neurodegeneration and
279 memory impairment (Nilsson *et al*, 2013). Besides increasing AKT phosphorylation, D4T also
280 significantly reduced the phosphorylation of another protein: ERK. Notably, whereas Ras-ERK
281 signaling induces A β and τ hyperphosphorylation, which is characteristically observed in AD
282 brains, p-ERK-p down regulation prevents τ and A β phosphorylation as well as neuronal cell cycle
283 entry (Kirouac *et al*, 2017). This complex link was further reinforced by recent results showing that
284 ERK phosphorylation is reduced in the presence of low A β concentrations (Kirouac *et al*, 2017).

285 Stavudine (D4T), an antiviral, has been used since the mid-80s in millions of HIV-infected
286 individuals (Fowler *et al*, 2014); this compound was shown to prevent caspase-1 activation and to
287 be efficient in mouse models of geographic atrophy, choroid neovascularization and graft-versus-
288 host disease (Fowler *et al*, 2014). Results herein indicating that D4T down regulates NLRP3
289 inflammasome activation and stimulates A β autophagy in an *in vitro* model of Alzheimer's disease
290 seem to warrant the investigation of its possible use in the clinical scenario.

291

292

293

294

295

MATERIALS AND METHODS

296

297

298 *Cells*

299 THP-1 human monocytes (IZSLER, Istituto Zooprofilattico Sperimentale della Lombardia e
300 Dell'Emilia Romagna, IT) were grown in RPMI 1640 supplemented with 10% FBS, 2mM L-
301 glutamine, and 1% penicillin (medium)(Invitrogen Ltd, Paisley, UK). To differentiate these cells
302 into macrophages, monocytes were seeded in 6-well plates at a density of 1.0×10^6 cells/well in
303 medium that contained 50 nM of phorbol 12-myristate 13-acetate (PMA)(Sigma-Aldrich, St. Louis,
304 MO) and incubated for 12 h at 37°C in 5% CO_2 ; cells were then resuspended in serum-free
305 medium.

306

307 *Cell culture*

308 THP-1-derived macrophages were cultured with medium alone or incubated with: 1) $\text{A}\beta_{42}$
309 ($10 \mu\text{g/ml}$)(Anaspec, Fremont, California, USA) for one hour, or 2) $\text{A}\beta_{42}$ after a 23 hours priming
310 with Lypopolissacaride (LPS) ($1 \mu\text{g/ml}$)(Sigma-Aldrich) in the absence/presence of D4T
311 ($50 \mu\text{M}$)(Sigma-Aldrich)(Lachlan R. Gray et al, 2013). Alexa Fluor 488 (FAM)-labeled $\text{A}\beta_{42}$ was
312 used in the phagocytosis assays and in ASC-speck detection; non-labeled $\text{A}\beta_{42}$ was used for gene-
313 expression and protein quantification.

314

315 *Cellular toxicity*

316 Viability of THP-1-derived macrophages was determined using the MTT 3-(4,5-dimethylthiazol-
317 2,5-diphenyltetrazolium bromide) (Sigma-Aldrich) assay, as previously described (Mossmann,
318 1983).

319

320 *RNA extraction and reverse transcription*

321 RNA was extracted from 1×10^6 THP-1-derived macrophages in unstimulated or stimulated
322 conditions (see above) in the absence/presence of D4T and reverse-transcribed into first-strand

323 cDNA (Biasin *et al*, 2010). Real-time PCR cDNA quantification was performed by real-time PCR
324 as previously described (Biasin *et al*, 2007).

325

326 ***NLRP3-Inflammasome and Trem2 gene expression***

327 NLRP3, ASC, Caspase-1, IL-1 β , IL-18 (Qiagen, Hilden, Germany) and TREM-2 (Sigma-Aldrich)
328 expression was evaluated by RT-PCR. Results were expressed as $\Delta\Delta C_t$ (where C_t is the cycle
329 threshold) and are presented as the ratio between the target gene and the GAPDH housekeeping
330 mRNA.

331

332 ***NLRP3-downstream inflammasome protein quantification by ELISA***

333 Proinflammatory cytokines were analyzed in supernatants of THP-1-derived macrophages in
334 unstimulated or stimulated conditions (see above) in the absence/presence of D4T. Caspase-1, IL-
335 1 β and IL-18 concentration was analyzed by sandwich immunoassays according to the
336 manufacturer's recommendations (Quantikine Immunoassay; R&D Systems, Minneapolis, MN,
337 USA). A plate reader (Sunrise, Tecan, Mannedorf, Switzerland) was used and optical densities
338 (OD) were determined at 450/620 nm. All the experiments were performed in triplicates. Sensitivity
339 (S) and Assay Range (AR) were as follows: S: IL-1 β =1pg/ml; Caspase-1= 1.24 pg/ml; IL-18= 12.5
340 pg/ml. AR: IL-1 β 3.9 -250 pg/ml; Caspase-1= 6.3 - 400 pg/ml; IL-18= 25.6- 1000 pg/ml.

341

342 ***AMNIS FlowSight analysis***

343 A β -FAM-phagocytosis, ASC-speck formation and NLRP3-complex assembly were analyzed by
344 FlowSight (Amnis Corporation, Seattle, WA). 1×10^6 in THP-1-derived macrophages stimulated
345 as described above. Cellswere fixed with 100 μ l of PFA (1%) (BDH, UK), permeabilized with 100
346 μ l of Saponine (0.1%) (Life Science VWR, Lutterworth, Leicestershire, LE) and stained with FITC-
347 anti human NLRP3 (Clone #768319, isotype Rat IgG2a, R&D Systems,) and PE-anti human ASC
348 (clone HASC-71, isotype mouse IgG1, Biolegend, San Diego, CA, USA) for 1 h at room

349 temperature. Cells were then washed with PBS, centrifuged at 1,500 rpm for 10 min and
350 resuspended in 50 μ l of PBS; results were analyzed by IDEAS analysis software (Amnis
351 Corporation, Seattle, WA, USA).

352 The FlowSight is an imaging flow cytometer that together merges flow cytometry and high-
353 resolution microscopy. It is equipped with two lasers operating at 488 and 642 nm, two camera and
354 twelve standard detection channels. It simultaneously produce side scatter (darkfield) image, one or
355 two transmitted light (brightfield) images, and up to ten channels of fluorescence imagery of every
356 cell. FlowSight using the Inspire™ system, acquires 2000 cells/second and operates with a 1 μ m
357 pixel size (~20X magnification) allowing visualization of fluorescence from the membrane,
358 cytoplasm, or nucleus; the IDEAS image analysis software allows quantification of the fluorescence
359 at different cellular localizations.

360 Phagocytosis assay were performed by internalization feature utilizing a mask representing the
361 whole cell, defined by the brightfield (BF) image, and an internal mask defined by eroding the
362 whole cell mask in order to eliminate the fluorescent signal coming from A β ₄₂-FAM attached to the
363 cell surface, thus measuring only the internalized part. The internalization feature was first used to
364 calculate the ratio of the intensity of FAM (A β ₄₂ signal) inside the cell/ total FAM intensity outside
365 the cell. Higher internalization scores indicate a greater concentration of A β ₄₂ FAM, inside the cell
366 (Supplementary Figure).

367 ASC-speck and NLRP3-inflammasome assembly analyses were performed using the same mask of
368 internalization feature, differentiating for ASC diffuse or spot (speck) fluorescence inside of cells
369 and its co-localization with the NLRP3 inflammasome protein.

370

371 ***Phagocytosis assay***

372 1×10^6 THP-1-derived macrophages were cultured with Alexa Fluor 488 (FAM)-labeled A β ₄₂ for 1h,
373 in unstimulated or stimulated conditions (see above) in the absence/presence of D4T. Medium
374 containing 0.05% Trypsin-EDTA (COD. ECB3052D, Euroclone, Milan, IT) was then added for 10
375 minutes at 37°C in 5% CO₂; to block trypsin, cells were then resuspended in RPMI 1640
376 supplemented with 10% FBS and centrifuged at 1500 rpm for 10 min. Pellet was fixed with 0.1%

377 paraformaldehyde (PFA) for 10 min, washed and resuspended in 50 μ l PBS. Supernatants were
378 collected and stored at -80°C for cytokine measurement by ELISA.

379

380 ***ERK1/2 and AKT quantification: total- and phospho-ELISA***

381 Phosphorylated ERK1/2 and AKT in lysates of THP-1-derived macrophages were analyzed using
382 Immunoassay Kits (phosphor-ELISA kits, BioSource International, Inc). Because total levels of
383 ERK1/2 and AKT are independent of phosphorylation status, total ELISA kits (BioSource) were
384 used to normalize the phosphorylated ERK1/2 and AKT content of the samples.

385 Protein cell extraction was performed in Cell Extraction Buffer (Biosource), containing 1mM
386 PMSF, protease and phosphatase inhibitor cocktail (Sigma-Aldrich)(1:200 and 1:100), for 30min,
387 on ice. Lysates were then centrifuged at 12000g for 10 minutes at 4°C. Different dilutions of
388 samples were tested for each phosphorylated or total protein detection. Protein absorbance was
389 determined at 450nm (BioRad); concentrations were calculated comparing absorbance to the
390 specific standard curve values for phosphorylated ERK and AKT, and expressed with respect to
391 each specific protein kinase total status.

392

393 ***Statistical analysis***

394 Experiments were repeated at least three times with triplicate of each condition. Firstly we
395 performed a parametric analysis of variance (one-way ANOVA) to evaluate phagocytosis and
396 cytokine production. Repeated measures ANOVA and Tukey post-test were performed for kinases
397 analyses. Results of ANOVA models are shown as means and SD (standard deviations). Post hoc
398 comparisons were run using t tests with Tuckey's HSD (honestly significant difference) procedure.
399 Data analysis was performed using the MedCalc and R statistical packages. Results were
400 considered to be statistically significant if surviving the $p < 0.05$ threshold.

401

402

403

404

405 **Acknowledgements**

406 This work was supported by 2017–2018 Ricerca Corrente (Italian Ministry of Health).

407

408 **Author contributions**

409 MC came up with the idea. FLR, MS and MC designed the experimental procedure. FLR, IM and
410 FP project performed the experiments. CPZ, EC and CF contributes reagents and useful insights.
411 ER performed statistical analyses. FLR, MS and MC wrote and edited the manuscript.

412

413 **Conflict of interest**

414

415 The authors declare that they have no conflict of interest.

416

417

418 **The paper explained**

419 **PROBLEM**In early phase of dementia, deposition of beta amyloid ($A\beta$) plaques induce
420 neuroinflammatory processes and the activation of immune system which include the activation of
421 microglia and the recruitment of peripheral monocytes in the AD brain. In particular, the
422 inflammasome has been implicated in several chronic inflammatory and autoimmune diseases and
423 recent data (*Halle 2008, Heneka 2013, Saresella 2016*) showed that NLRP3, an inflammasome
424 component, is activated in AD. NLRP3 activation leads to production of the proinflammatory
425 cytokines IL-1 β , IL-18 and caspase-1 resulting in inflammatory milieu that reduce $A\beta$ -clearance
426 and down-regulation of TREM2 (*Thornton 2017*) a receptor protein that allows microglia to
427 phagocyte $A\beta$.

428

429 **RESULTS**

430 Recent data show that nucleoside reverse transcriptase inhibitors (NRTI) are endowed with an
431 intrinsic anti-inflammatory activity as they inhibit the assembly of the inflammasome. Given these
432 data, we hypothesize that the administration of NRTI and in particular Stavudine (an oral compound
433 that has been used for years in HIV infection) blocking NLRP3 assembly, could prevent caspase-1
434 activation and, as a consequence, IL-18 release; this could block inflammasome, or could
435 polarize monocytes to an anti-inflammatory phenotype, restoring phagocytosis functions. We
436 propose that this drug could be an interesting tool in the treatment of AD.

437

438 **IMPACT**

439 An in-depth analysis of the possible beneficial effects of component that suppress inflammasome
440 NLRP3 activation in AD (NRTI-stavudine).

441

442

Supplementary data

443

444 A β ₄₂-phagocytosis detection by FlowSight specifically shows single cell events that were identified
445 using a dot plot of brightfield (BF) Aspect Ratio *versus* BF Area Aspect Ratio is a feature value
446 calculated by dividing the height of the cell by the width. On the FlowSight single cell events tend
447 to have an aspect ratio between 0.7 and 1.0. On the basis of macrophages a second plot, using A β -
448 internalization score (IS) was generated to identify the percentage of THP-1-derived macrophages
449 were positive for A β -FAM relative to the negative control A positive value of IS corresponds to a
450 cell with mostly A β -internalized, represents the ratio of fluorescence intensity inside the cell to the
451 total fluorescence intensity of the cell and identifies the phagocytic capacity of the cells.

452

453 Supplementary figure: Determination of A β phagocytosis by macrophage derived THP-1 cell line;

454 Representative images capture by Amnis Flow Sight Cytometry of cells untreated (negative control)
455 or stimulated with Alexa Fluor 488-labeled A β (FAM-A β); In panel A are shown gated
456 macrophages image (left) based on Area and Aspect Ratio: area of the cell were identified as
457 number of pixels and converted to μm^2 (1 pixel = 0.25 μm^2); image of percentage of FAM-A β
458 positive macrophages (positive control) is shown (right). In panel B is shown brightfield (BF)
459 image (left) of negative cell for Alexa Fluor 488 fluorescence (right). In panel C: first column
460 shows BF image of macrophages treated with FAM-A β (a), second column shows image related to
461 FAM-A β fluorescence (b), third column shows merged fluorescence with BF (c). Internalization
462 score (IS) calculated by IDEA software is shown (d). Scale bar 20 μm .

463

464

465

466

467

468

469

REFERENCES

- 470
471
472 Awad F, Assrawi E, Jumeau C, Georgin-Lavialle S, Cobret L, Duquesnoy P, Piterboth W,
473 Thomas L (2017) Impact of human monocyte and macrophage polarization on NLR
474 expression and NLRP3 inflammasome activation. *Plos one* 12;12(4):e0175336
475 Bajramovic JJ (2011) Regulation of innate immune responses in the central nervous system.
476 *CNS & neurological disorders drug targets* 10: 4-24
477 Biasin M, Piacentini L, Lo Caputo S, Naddeo V, Pierotti P, Borelli M, et al. TLR activation
478 pathways in HIV-1-exposed seronegative individuals (2010) *J Immunol* 184:2710–2717
479 Biasin M, Piacentini L, Lo Caputo S, Kanari Y, Magri G, Trabattoni D, Naddeo V, Lopalco
480 L, Clivio A, Cesana E, Fasano F, Bergamaschi C, Mazzotta F, Miyazawa M, Clerici M
481 (2007) Apolipoprotein B mRNA-editing enzyme, catalytic polypeptide-like 3G: a possible
482 role in the resistance to HIV of HIV-exposed seronegative individuals. *J Infect Dis* 195:960–
483 964.
484 Bouchon A, Hernandez-Munain C, Cella M, Colonna M (2001) DAP12-mediated pathway
485 regulates expression of CC chemokine receptor 7 and maturation of human dendritic cells. *J*
486 *Exp Med* 194: 1111-1122.
487 Cai Z, Hussain MD, Yan LJ (2014) Microglia, neuroinflammation, and beta-amyloid protein in
488 Alzheimer's disease. *Int J Neurosci* 124(5):307-21.
489 Casati M, Ferri E, Gussago C, P. Mazzolad, Abbatec C, Bellellid G, Maria D, Cesaria M and
490 Arosio B (2018) Increased expression of TREM2 in peripheral cells from mild cognitive
491 impairment patients who progress into Alzheimer's disease. *European Journal of Neurology*
492 25(6):805-810
493 Colonna M and Wang Y (2016) TREM2 variants: new keys to decipher Alzheimer
494 diseaspathogenesis *Nat Rev Neurosci* 17(4):201-7
495 Dempsey C, Rubio Araiz A, Bryson KJ, Finucane O, Larkin C, Mills EL, Robertson AA, Cooper
496 MA, O'Neill LAJ, Lynch MA (2017) Inhibiting the NLRP3 inflammasome with MCC950
497 promotes non-phlogistic clearance of amyloid- β and cognitive function in APP/PS1 mice.
498 *Brain Behav Immun* 61:306-316.
499 Feng Y, Li L, Sun XH (2011) Monocytes and Alzheimer's disease. *Neurosci Bull* 2, 115-122.
500 Ferguson TA and Green TR (2014) Autophagy and phagocytosis converge for better
501 vision. *Autophagy* 10(1): 165–167
502 Fiala MJ, Ringman LJ, Kermani-Arab V, Tsao G, Patel A, Lossinsky A, Graves MC, Gustavson
503 A, Sayre J, Sofroni E, Suarez T, Chiappelli F and Bernard G (2005) Ineffective phagocytosis

504 of amyloid-beta by macrophages of Alzheimer's disease patients. *Journal of Alzheimer's*
505 *Disease* 7 221–232

506 Fowler BJ, Gelfand BD, Kim Y, Kerur N, Tarallo V, Hirano Y, Amarnath S, Fowler DH,
507 Radwan M, Young MT, Pittman K, Paul Kubes Agarwal HK, Parang K, Hinton DR, Bastos-
508 Carvalho A, Li S, Yasuma T, Mizutani T, Yasuma R, et al (2014) Ambati^{1,2} Nucleoside
509 reverse transcriptase inhibitors possess intrinsic anti-inflammatory activity. *Science*
510 346(6212):1000-3.

511 Gaidt MM, Ebert TS, Chauhan D, Cooper MA, Graf T, Hornung V (2016) Human Monocytes
512 Engage an Alternative Inflammasome Pathway. *Immunity* 44, 833–846

513 Griffin WS, Liu L, Li Y, Mrak RE, Barger SW. Interleukin-1 mediates Alzheimer and Lewy
514 body pathologies. *J Neuroinflammation*. 2006;3:5–9

515 Haitao Guo, Justin B. Callaway, and Jenny P.-Y. Ting. Inflammasomes: Mechanism of Action,
516 Role in Disease, and Therapeutics. *Nat Med*. 2015 July ; 21(7): 677–687

517 Halle A, Hornung V, Petzold GC, Stewart CR, Monks BG, Reinheckel T, Fitzgerald KA, Latz
518 E, Moore KJ, Golenbock DT (2008) The NALP3 inflammasome is involved in the innate
519 immune response to amyloid-beta. *Nat Immunol* 9(8):857–65

520 Hamerman JA, Jarjoura JR, Humphrey MB, Nakamura MC, Seaman WE, Lanier LL (2006)
521 Cutting edge: inhibition of TLR and FcR responses in macrophages by triggering receptor
522 expressed on myeloid cells (TREM)-2 and DAP12. *Journal of immunology* 177: 2051-2055

523 Harris J, Hartman M, Roche C, Zeng SG, O'Shea A, Sharp FA (2011) Autophagy controls IL-
524 1beta secretion by targeting pro-IL-1beta for degradation. *J Biol Chem* 286:9587-97

525 Heneka MT, Carson MJ, Khoury J, Landreth GE, Brosseron F, Feinstein DL, Jacobs AH,
526 Wyss-Coray T, Vitorica J, Ransohoff RM (2015a) Neuroinflammation in Alzheimer's
527 disease. *Lancet Neurol* 14:388–405

528 Heneka MT, Kummer MP, Stutz A, Delekate A, Schwartz S, Vieira-Saecker A, Griep A, Axt
529 D, Remus A, Tzeng TC, Gelpi E, Halle A, Korte M, Latz E, Golenbock DT (2013) NLRP3
530 is activated in Alzheimer's disease and contributes to pathology in APP/PS1 mice. *Nature*
531 493(7434):674-8

532 Heras-Sandoval D, Ferrera P, Arias C (2012) Amyloid- β protein modulates insulin signaling in
533 presynaptic terminals. *Neurochem Res* 37(9):1879-85.

534 Hui IQ, Asadi A, Park JY, Kieffer TJ, Ao Z, Warnock GL, Marzban L (2017) Amyloid
535 formation disrupts the balance between interleukin-1b and interleukin-1 receptor antagonist
536 in human *Molecular Metabolism* 31;6(8):833-844

- 537 Hu X, Leak RK, Shi Y, Suenaga J, Gao Y, Zheng P and Chen J (2015) Microglial and
538 macrophage polarization-new prospects for brain repair *Nat Rev Neurol. Nat Rev Neurol*
539 11(1): 56–64
- 540 Jin P, Choi DY, Hong JT (2012) Inhibition of extracellular signal-regulated kinase activity
541 improves cognitive function in Tg2576 mice *Clin Exp Pharmacol Physiol* 39(10):852-857
- 542 Joassard OR, Amirouche A, Gallot YS, Desgeorges MM, Castells J, Durieux AC, Berthon
543 P, Freyssenet DG (2013) Regulation of Akt-mTOR, ubiquitin-proteasome and autophagy-
544 lysosome pathways in response to formoterol administration in rat skeletal muscle. *Int J*
545 *Biochem Cell Biol* 45(11):2444-55
- 546 Jones BM, Bhattacharjee S, Dua P, Hill JM, Zhao Y, Lukiw W (2014) Regulating
547 amyloidogenesis through the natural triggering receptor expressed in myeloid/microglial
548 cells 2 (TREM2). *Front Cell Neurosci* 31;8:94
- 549 Kerur N, Hirano Y, Tarallo V, Fowler BJ, Bastos-Carvalho A, Yasuma T, Yasuma R, Kim
550 Y, Hinton DR, Kirschning CJ, Gelfand BD, Ambati J (2013) TLR-independent and P2X7-
551 dependent signaling mediate Alu RNA-induced NLRP3 inflammasome activation in
552 geographic atrophy. *Invest Ophthalmol Vis Sci* 54(12):7395-401
- 553 Kiffin R, Christian C, Knecht E, Cuervo AM (2004) Activation of chaperone-mediated
554 autophagy during oxidative stress. *Mol Biol Cell* 15(11):4829-40
- 555 Kirouac L, Rajic AJ, Cribbs DH, and Padmanabhan J (2017) Activation of Ras-ERK Signaling
556 and GSK-3 by Amyloid Precursor Protein and Amyloid Beta Facilitates Neurodegeneration
557 in Alzheimer's Disease. *eNeuro.* 27;4(2)
- 558 Klesney-Tait J, Turnbull IR, Colonna M (2006) The TREM receptor family and signal
559 integration. *Nature immunology* 7: 1266-1273
- 560 La Rosa F, Saresella M, Baglio F, Piancone F, Marventano I, Calabrese E, Nemni R,
561 Ripamonti E, Cabinio M, Clerici M (2017) Immune and Imaging Correlates of Mild
562 Cognitive Impairment Conversion to Alzheimer's Disease. *Scientific reports* n°16760
- 563 Lamkanfi M, Walle VL and Kanneganti TD (2011) Deregulated inflammasome signaling in
564 disease. *Immunol Rev* 243(1): 163–173.
- 565 Li Y, Lu L, Luo N1, Wang YQ, Gao HM (2017) Inhibition of PI3K/Akt/mTOR signaling
566 pathway protects against d-galactosamine/lipopolysaccharide-induced acute liver failure by
567 chaperone-mediated autophagy in rats. *Biomed Pharmacother* 92:544-553
- 568 Lupfer C, Thomas PG, Anand PK, Vogel P, Milasta S, Martinez J, Huang G, Green M, Kundu
569 M, Chi H, Xavier RJ, Green DR, Lamkanfi M, Dinarello CA, Doherty PC, Kanneganti TD

- 570 (2013) Receptor interacting protein kinase2-mediated mitophagy regulates inflammasome
571 activation during virus infection. *Nat. Immunol* 14:480–88
- 572 Maiké Gold and Joseph El Khoury (2015) β -amyloid, Microglia and the Inflammasome in
573 Alzheimer's Disease *Semin Immunopathol* 37(6): 607–611
- 574 Martínez-López N, Athonvarangkul D, Mishall P, Sahu S, Singh R (2013) Autophagy proteins
575 regulate ERK phosphorylation. *Nat Commun* 4:2799
- 576 Mezzasoma L, Antognelli C, Talesa VN (2017) A Novel Role for Brain Natriuretic Peptide:
577 Inhibition of IL-1 β Secretion via Downregulation of NF-kB/Erk 1/2 and
578 NALP3/ASC/Caspase-1 Activation in Human THP-1 Monocyte. *Mediators Inflamm.*
579 2017:5858315.
- 580 N. Hay (2005) The Akt-mTOR tango and its relevance to cancer. *Cancer Cell* 8:179-183
- 581 Nakahira K, Haspel JA, Rathinam VA, Lee SJ, Dolinay T, Lam HC, Englert JA, Rabinovitch
582 M, Cernadas M, Kim HP, Fitzgerald KA, Ryter SW, Choi AM (2011) Autophagy proteins
583 regulate innate immune responses by inhibiting the release of mitochondrial DNA mediated
584 by the NALP3 inflammasome. *Nat. Immunol.* 12:222–30
- 585 Netea MG, Nold-Petry CA, Nold MF, Joosten LAB, Opitz B, van der Meer JHM, van de
586 Veerdonk FL, Ferwerda G, Heinhuis B, Devesa I, Funk CJ, Mason RJ, Kullberg BJ,
587 Rubartelli A, van der Meer JWM, and Dinarello CA (2009) Differential requirement for the
588 activation of the inflammasome for processing and release of IL-1 β in monocytes and
589 macrophages. *Blood* 113(10): 2324–2335
- 590 Neumann H and Takahashi K (2007) Essential role of the microglial triggering receptor
591 expressed on myeloid cells-2 (TREM2) for central nervous tissue immune homeostasis.
592 *Journal of neuroimmunology* 184: 92-99
- 593 Nilsson P, Loganathan K, Sekiguchi M, Matsuba Y, Hui K, Tsubuki S, Tanaka M, Iwata N, Saito
594 T and Saido TC (2013) A β Secretion and Plaque Formation Depend on Autophagy. *Cell*
595 *Reports* 5, 61–69
- 596 Parajuli B, Sonobe Y, Horiuchi H, Takeuchi H, Mizuno T, and Suzumura A (2013)
597 Oligomeric amyloid β induces IL-1 β processing via production of ROS: implication in
598 Alzheimer's disease *Cell Death Dis* 4(12): e975
- 599 Peng DJ, Wang J, Zhou J, Yand Wu GS (2010) Role of the Akt/mTOR survival pathway in
600 cisplatin resistance in ovarian cancer cells. *Biochem Biophys Res Commun* 394(3): 600–605
- 601 Qian S, Fan J, Billiar TR and Scott MJ (2017) Inflammasome and Autophagy Regulation: A
602 Two-way Street. *Mol Med* 23: 188–195

- 603 Ravindran R, Loebbermann J, Nakaya HI, Khan N, Ma H, Gama L, Machiah DK, Lawson
604 B, Hakimpour P, Wang YC, Li S, Sharma P4, Kaufman RJ, Martinez J, Pulendran B (2016).
605 The amino acid sensor GCN2 controls gut inflammation by inhibiting inflammasome
606 activation. *Nature* 531:523–27
- 607 Rodgers MA, Bowman JW, Liang Q, Jung JU (2014) Antioxid Redox Signal.Regulation where
608 autophagy intersects the inflammasome 20(3):495-506
- 609 Saitoh T, Akira S Regulation of inflammasomes by autophagy (2016) *J Allergy Clin Immunol*
610 138(1):28-36
- 611 Saresella M, La Rosa F, Piancone F, Zoppis M, Marventano I, Calabrese E, Rainone V, Nemni
612 R, Mancuso R, Clerici M (2016) The NLRP3 and NLRP1 inflammasomes are activated in
613 Alzheimer's disease. *Mol Neurodegener* 3;11:23
- 614 Shi CS, Shenderov K, Huang NN, Kabat J, Abu-Asab M, Fitzgerald KA, Sher A, and Kehrl JH
615 (2012) Activation of Autophagy by Inflammatory Signals Limits IL-1 β Production by
616 Targeting Ubiquitinated Inflammasomes for Destruction. *Nat Immunol* 13(3): 255–263
- 617 Shibutani ST , Saitoh T, Nowag H, Münz C, Yoshimori T (2015) Autophagy and autophagy-
618 related proteins in the immune system. *Nat Immunol* 16(10):1014-24
- 619 Simard AR, Soulet D, Gowing G, Julien JP, Rivest S (2006) Bone marrow-derived microglia
620 play a critical role in restricting senile plaque formation in Alzheimer's disease. *Neuron* 4,
621 489-502
- 622 Strowig T, Henao-Mejia J, Elinav E, Flavell R (2012) Inflammasomes in health and disease.
623 *Nature* 481(7381):278-86
- 624 Tan J, Town T, Abdullah L, Wu Y, Placzek A, Small B, Kroeger J, Crawford F, Richards D,
625 Mullan M (2002) CD45 isoform alteration in CD4+ T cells as a potential diagnostic marker
626 of Alzheimer's disease. *J Neuroimmunol* 132, 164- 17
- 627 Tan YJ, Ng ASL, Vipin A, Lim JKW, Chander RJ, Ji F, Qiu Y, Ting SKS, Hameed S, Lee
628 TS, Zeng L, Kandiah N, Zhou J (2017) Higher Peripheral TREM2 mRNA Levels Relate to
629 Cognitive Deficits and Hippocampal Atrophy in Alzheimer's Disease and Amnesic Mild
630 Cognitive Impairment. *Journal of Alzheimer's disease. JAD* 58: 413-423
- 631 Town T, Tan J, Mullan M (2001) CD40 signaling and Alzheimer's disease pathogenesis.
632 *Neurochem Int* 39, 371- 380
- 633 Town T, Nikolic V, Tan J (2005) The microglial "activation" continuum: From innate to
634 adaptive responses. *J Neuroinflammation* 31, 2-24

- 635 Town T, Laouar Y, Pittenger C, Mori T, Szekely CA, Tan J, Duman RS, Flavell RA (2008)
636 Blocking TGF-beta-Smad2/3 innate immune signaling mitigates Alzheimer-like pathology.
637 Nat Med 14, 681-687
- 638 Townsend KP, Town T, Mori T, Lue LF, Shytle D, Sanberg PR, Morgan D, Fernandez F,
639 Flavell RA, Tan J (2005) CD40 signaling regulates innate and adaptive activation of
640 microglia in response to amyloid beta-peptide. Eur J Immunol 35, 901- 910
- 641 Tuppo EE and Ariasb HR (2005) The role of inflammation in Alzheimer's disease The
642 International Journal of Biochemistry & Cell Biology 37:289–305.
- 643 Uddin MS, Stachowiak A, Mamun AA, Tzvetkov NT, Takeda S,Atanasov AG, Bergantin
644 LB,Abdel-Daim MM and Stankiewicz AM (2018) Autophagy and Alzheimer'sDisease:
645 From Molecular Mechanisms to Therapeutic Implications.Front. Aging Neurosci10:4
646
- 647 Vernon PJ and Tang D (2013) Eat-Me: Autophagy, Phagocytosis, and Reactive Oxygen
648 Species Signaling. Antioxidants &Signaling 18(6).
- 649 Wang D, Xu N, Zhang Z, Yang S, Qiu C, Li C, Deng G, Guo M (2016) Retraction notice to
650 Sophocarpine displays anti-inflammatory effect via inhibiting TLR4 and TLR4 downstream
651 pathways on LPS-induced mastitis in the mammary gland of mice. Int Immunopharmacol
5:111-118
- 652 Yang Z and Klionsky DJ (2010) Eaten alive: a history of macroautophagy. Nat Cell Biol
653 12(9):814-22.
654
- 655 Zuroff L, Daley D, Black KL, Koronyo-Hamaoui M. (2017) Clearance of cerebral A β in
656 Alzheimer's disease: reassessing the role of microglia and monocytes. Cell Mol Life Sci
74(12):2167-2201

657

658

659

660

661

662

663

664

665

666

667

Figures legends

668

669 **Figure 1: *Inflammasome pathway mRNA expression and in stimulated macrophage derived***
670 ***THP-1 cell line***; Single real-time PCR results obtained in cells cultured alone with A β (10 μ g/ml)
671 or primed with lipopolysaccharide (LPS) (1 μ g/ml) and A β with or without D4T. Genes of
672 inflammasome proteins: IL-1 β , caspase1, IL-18, NLRP3 and ASC are shown in the panels A-F.
673 Gene expression was calculated relative to GAPDH housekeeping gene. The results are indicated as
674 fold-change expression from the unstimulated samples. Summary results, obtained using the TIGR
675 Multi Experiment Viewer (MeV)v4.9, are shown in the bar graphs in panel G.

676

677 **Figure 2: *Modulation of NLRP3 inflammasome effector proteins by D4T in stimulated***
678 ***macrophage derived THP-1 cell line***; Cytokines IL-1 β (panel A), Caspase 1 (panel B), and IL-18
679 (panel C) production was measured by ELISA on supernatants of THP-1 cells treated with A β -
680 alone (10 μ g/ml) or primed with lipopolysaccharide (LPS) (1 μ g/ml) and/or with D4T (50 μ M). Data
681 are representative of three independent experiments and expressed as means \pm SD. Untreated cells
682 condition was indicated as medium. Statistical significance is shown.

683

684 **Figure 3: *NLRP3/ASC-speck formation in treated macrophage derived THP-1 cell line.***
685 NLRP3/ASC-speck colocalization was analyzed by Amnis Flow Sight Cytometry. 1*10⁶ cells
686 treated with A β alone (10 μ g/ml) (panel A), or after inflammasome activation with
687 lipopolysaccharide (LPS) (1 μ g/ml) and A β ₄₂ (LPS+A β) (panel B) or after D4T treatment (panel C).
688 In all panels: the first column shows cells in brightfield (BF), second column shows NLRP3-FITC
689 fluorescence, third column shows ASC-PE fluorescence, and fourth column shows florescence of
690 ASC merged with NLRP3. Results were summarized as percentage of positive cells for
691 NLRP3/ASC-speck in LPS+A β compared to A β and/or with D4T stimulated cells (IDEA software)
692 (panel D). Statistical significance is shown. Scale bar 20 μ m.

693 **Figure 4: *AMNIS FlowSight analysis of percentage for FAM-A β positive macrophage derived***
694 ***THP-1 cell line***;The phagocytic ability of THP-1-derived macrophages were measured in all
695 experimental conditions; 1x10⁶ macrophage were treated only with FAM-A β or after
696 inflammasome activation with lipopolysaccharide (LPS) (1 μ g/ml) and FAM-A β (LPS+ A β) (panel
697 A) and/or with D4T treatment (panel B). Data were shown as mean \pm SD of three independent
698 experiments; statistical significance is indicated.

699 **Figure 5: *TREM-2* expression in macrophage derived THP-1 cell line;** mRNA expression by
700 single real-time PCR; results are indicated as fold-change expression from the unstimulated samples
701 and calculated relative to GAPDH housekeeping gene. Statistical significance is shown.

702
703 **Figure 6: *Autophagy kinases modulate NLRP3* in macrophage derived THP-1 cell line;**
704 phosphorylation status of ERK (A) and AKT (B) kinases was assessed by phospho(P)-ELISA in
705 cytosol protein extracts of unstimulated cells or lipopolysaccharide (LPS) (1 μ g/ml) and A β
706 stimulated cells and/or with D4T treatment. Data were analyzed by ANOVA and is depicted as
707 mean \pm SD of three independent experiments; significant difference from cells untreated is shown.

708

709

710

711

712

713

714

715

716

717

718

719

720

721

722

723

724

Figure 1

bioRxiv preprint doi: <https://doi.org/10.1101/377945>; this version posted July 26, 2018. The copyright holder for this preprint (which was not certified by peer review) is the author/funder, who has granted bioRxiv a license to display the preprint in perpetuity. It is made available under aCC-BY-NC-ND 4.0 International license.

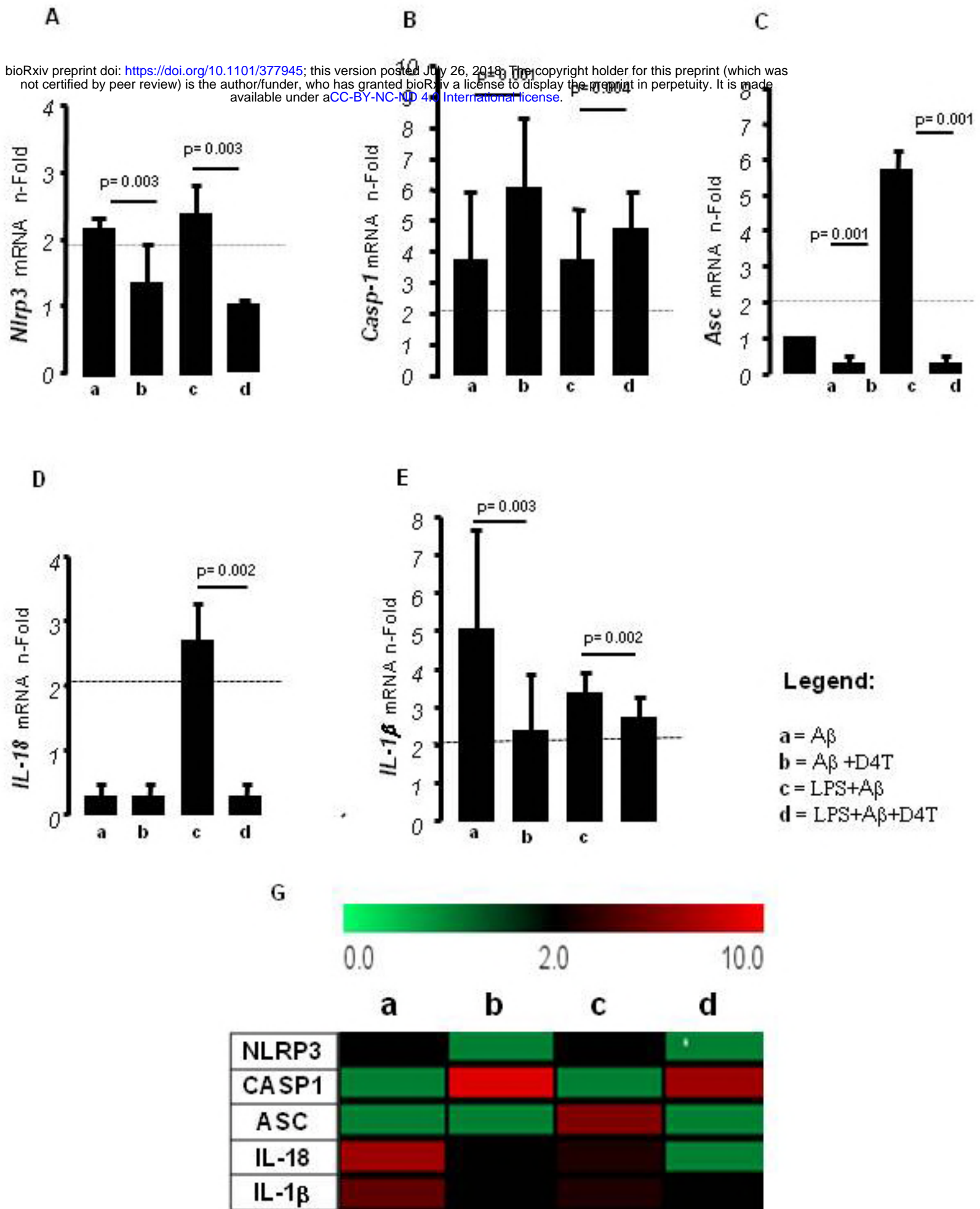


Figure 2

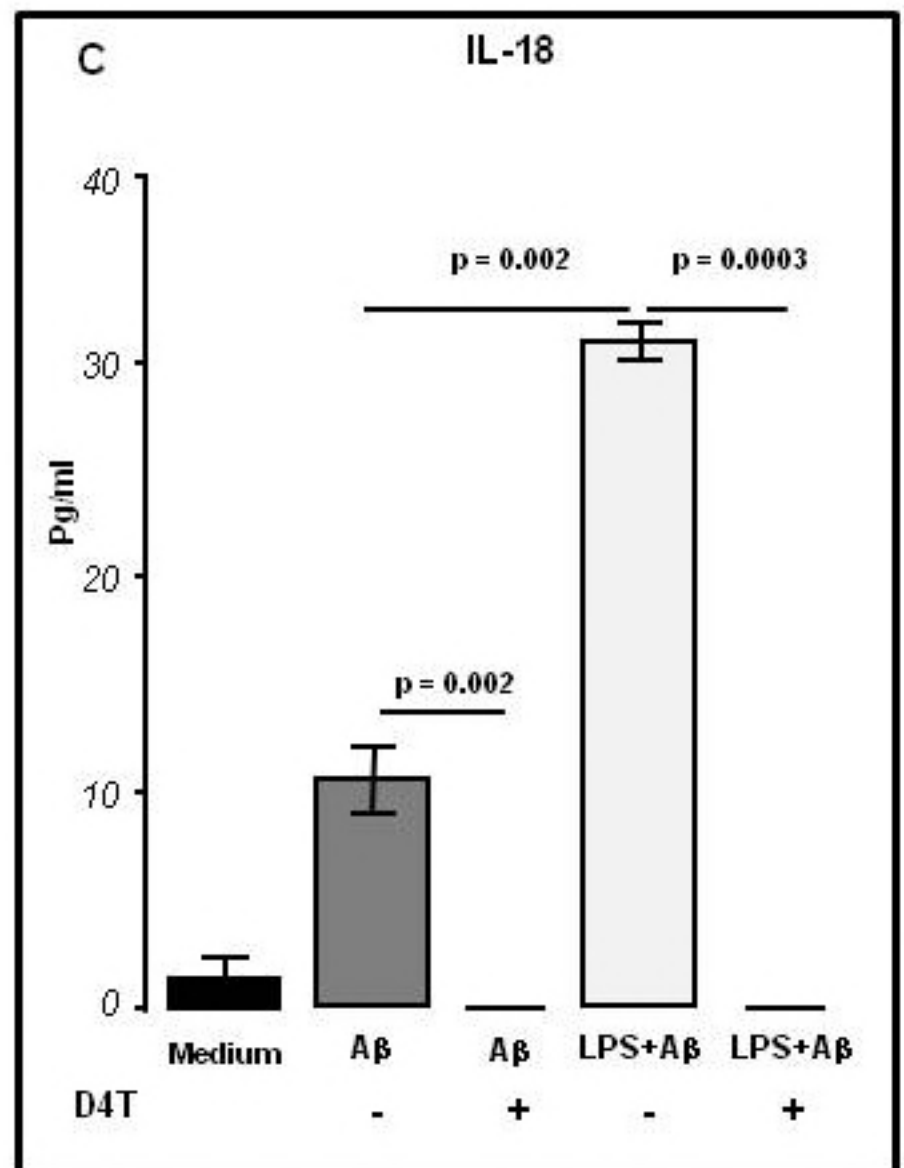
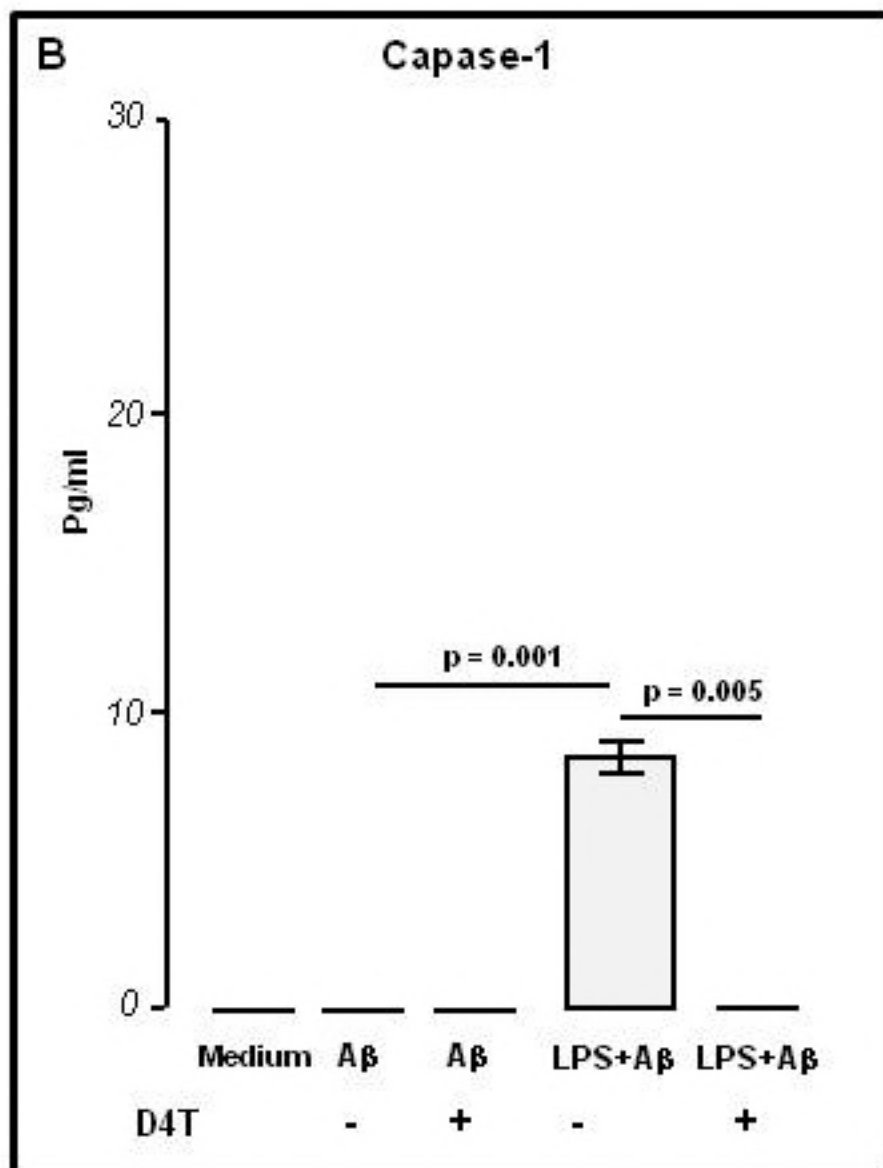
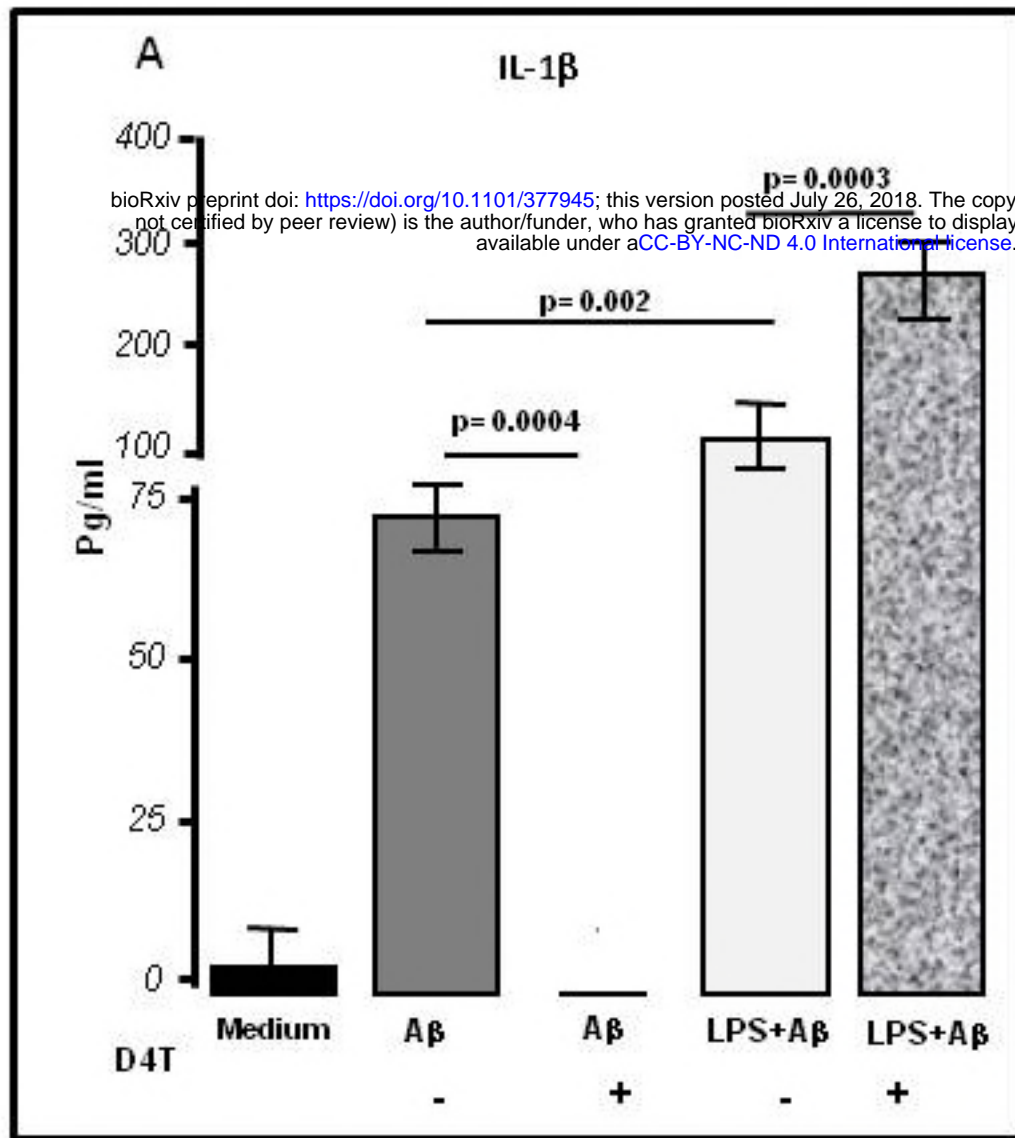


Figure 3

bioRxiv preprint doi: <https://doi.org/10.1101/377945>; this version posted August 20, 2019. The copyright holder for this preprint (which was not certified by peer review) is the author/funder, who has granted bioRxiv a license to display the preprint in perpetuity. It is made available under aCC-BY-NC-ND 4.0 International license.

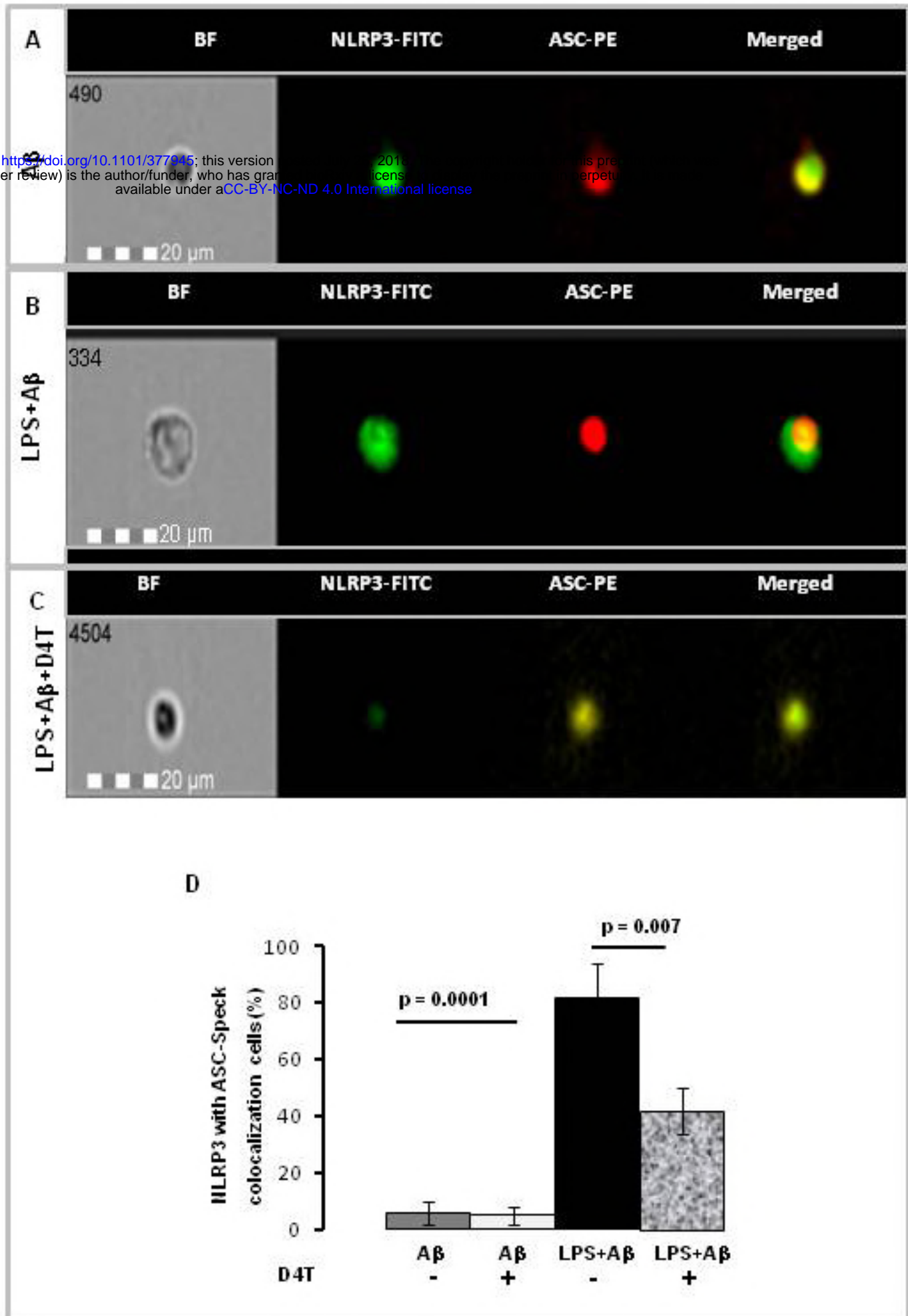


Figure 4

